Remote metastasis detection by video thermometry: A promissing preclinical study

Paula Gebe Abreu Cabral (pgacabral99@gmail.com)
Department of Clinical Surgery Veterinary Hospital, Animal Experimental Unit, UENF, 2000 Alberto Lamego avenue, Campos dos Goytacazes, Rio de Janeiro, Brazil https://orcid.org/0000-0002-4405-6511

Silvia Marcela Ruiz Cadena
Department of Clinical Surgery Veterinary Hospital, Animal Experimental Unit, UENF, 2000 Alberto Lamego avenue, Campos dos Goytacazes, Rio de Janeiro, Brazil

Scarlath Ohana Penna dos Santos
Department of Clinical Surgery Veterinary Hospital, Animal Experimental Unit, UENF, 2000 Alberto Lamego avenue, Campos dos Goytacazes, Rio de Janeiro, Brazil

Sávio Bastos de Souza
Galzu Institute, Santa Casa de Misericórdia de Campos Hospital, 115 pelinca avenue, Campos dos Goytacazes, Rio de Janeiro, Brazil https://orcid.org/0000-0003-3169-7309

José Edgard De Oliveira Alves
Department of anaesthesiology and pharmacology, UENF, 2000 Alberto Lamego avenue, Campos dos Goytacazes, Rio de Janeiro, Brazil

Jussara Peters Scheffer
Department of Clinical Surgery Veterinary Hospital, Animal Experimental Unit, UENF, 2000 Alberto Lamego avenue, Campos dos Goytacazes, Rio de Janeiro, Brazil

Hassan Jerdy Leandro
Department of animal morfology and pathology, UENF, 2000 Alberto Lamego avenue, Campos dos Goytacazes, Rio de Janeiro, Brazil

Gustavo D'annunciação Braga
Department of Clinical Surgery Veterinary Hospital, Animal Experimental Unit, UENF, 2000 Alberto Lamego avenue, Campos dos Goytacazes, Rio de Janeiro, Brazil

Renato Martins da Silva
Galzu Institute, Santa Casa de Misericórdia de Campos Hospital, 115 pelinca avenue, Campos dos Goytacazes, Rio de Janeiro, Brazil

Raul Ferraz Arruda
Galzu Institute, Santa Casa de Misericórdia de Campos Hospital, 115 pelinca avenue, Campos dos Goytacazes, Rio de Janeiro, Brazil

Sheila Passos de Figueiredo Cabral
Galzu Institute, Santa Casa de Misericórdia de Campos Hospital, 115 pelinca avenue, Campos dos Goytacazes, Rio de Janeiro, Brazil

Fernanda Antunes
Department of anaesthesiology and pharmacology, UENF, 2000 Alberto Lamego avenue, Campos dos Goytacazes, Rio de Janeiro, Brazil
André Lacerda de Abreu Oliveira (lacerdavet@uol.com.br)
Coordinator of Animal Experimental Unit, Department of Clinical Surgery Veterinary Hospital, North Fluminense Estatal University (UENF), 2000 Alberto Lamego avenue, Rio de Janeiro, Campos dos Goytacazes, Brazil

---

Research Article

Keywords: breast cancer, diagnostic imaging, video thermometry, infrared imaging, SaMD

Posted Date: June 28th, 2023

DOI: https://doi.org/10.21203/rs.3.rs-3115452/v1

Abstract

The thermometric video image (VTM) can guide the search for distant metastases, once the vascular architecture is known, identifying, by segmentation, the tumor thermal impression and a similar pattern at a distance. Thus, suspicious areas can be better investigated, improving the postoperative prognosis. In this study, it was possible to observe the assertive capacity of video thermometry in identifying distant metastases and breast tumors in female dogs, not palpable or visible to the naked eye, in relation to conventionally used techniques. It was also possible to identify textures with anatomical limits, from emboli to early formations of carcinomas, adenocarcinomas and adenomyoepithelioma. It was also possible to find non-neoplastic changes such as dermatitis, lipoma, hyperplasia and breast cysts. it can be concluded that the video thermometry (VTM) technique was capable of identifying distant metastases from the primary tumor and other benign alterations with great precision. However, for this to be possible, it is essential that the processing be carried out by SaMD (Software as a Medical Device), with tools capable of identifying patterns and thermal signatures, just like the algorithm, thus increasing the efficacy of the technique.

1. INTRODUCTION

Approximately 25% of female dogs develop new nodules following surgical removal, which have the potential to be malignant despite the initial tumor being benign[1]. The process of metastasis is selective for the few cells that lose their adhesion and manage to penetrate vessel walls, eventually forming emboli in distant capillary beds. If the immune system fails to eliminate these cells, metastasis can occur[2]. Angiogenesis, hypervascularity, and hyperthermia are frequent and early alterations observed in breast tumors[3,4,5], small with only 100 cells[6]. Furthermore, the extracellular space in most tumors is slightly acidic due to the excessive production of lactic acid (aerobic glycolysis - chronic activation of hypoxia-inducible factor-1 / HIF-1) and the H^+ transport through the plasma membrane mediated by V-ATPases[7,8]. This acidity creates a favorable tumor microenvironment, promoting angiogenesis and influencing its invasive capabilities[9]. However, the hypervascularity and microvessel density around the tumor correlate with the central temperature of the tumor[10], and this heat is a result of different metabolic intensities[11] It can be detected by infrared sensors[12,13].

In 1957, a milestone in the detection of breast cancer occurred when Lawson used, for the first time, a thermal camera for this purpose. He identified temperature differences between the tumor and the surrounding healthy area. In 1963, researchers such as Lausanne and Ghatmati published studies that associated increased skin temperature with breast cancer, highlighting the importance of venous convection in this process. In 1982, the Food and Drug Administration (FDA) approval thermometry as a diagnostic aid to detect breast cancer ~~came~~. In 1996, a comparative study between thermal imaging and radiography showed that thermal imaging was able to detect the disease in a patient, while radiography was not able to identify it.[14]. Subsequently, in 2003, the FDA approved real-time digital thermometry as a classifier for assisted neural networks.

Different tissues have different emissivity at infrared wavelengths, emitting signals[15,16]. Objects naturally emit thermal signals in the range of infrared electromagnetic radiation, and the type of signal emitted or radiated at a certain temperature depends on both the characteristics of the object and its surrounding environment[17], just like the technology that captures these signals and transforms them into images[18], Therefore, infrared measurement devices acquire the radiation emitted by the object and convert it into an electronic signal[19,20]. When a cell performs a biological task ATP hydrolysis takes place resulting in the loss of energy in the form of heat[21]. Only with the advancements in thermodynamics was the mechanical theory of heat established, with heat being recognized as dynamic energy in motion, derived from molecular motion based on the degree of freedom of each molecule[22], which can be measured on a varying scale of degrees that we refer to as temperature[23]. The heat from infrared radiation is based on thermodynamics and the transfer of bioheat[24]. The Stefan-Boltzmann law can be used to understand the relationship between the energy emitted by an object and its temperature, while the Penne's bioheat equation can effectively measure the heat produced by cancer cells.[25]. In breast carcinomas, increased cellular activity leads to changes in local temperature[26] As a result, the heat generated from metabolism can vary in intensity, leading to thermal asymmetries[27].

Infrared electromagnetic radiation lies outside the human visual range and, therefore, is capable of recording non-visible occurrences[28]. On the other hand, the sensitivity of infrared sensors has significantly improved from 0.5°C in the 1960s to less than 0.02°C in modern sensors, allowing them to accurately capture the subtle temperature variations of the breast[29]. The dynamic cooling-assisted video image capture monitors the temperature of each pixel over time, thereby increasing specificity[30], furthermore, with computational resources, artificial intelligence can be utilized to extract more features from this technology[31]. Although, the use of thermography has been recognized as a potential mechanism for the diagnosis and monitoring of cancers, particularly skin and breast cancers, thermography is linked to portable cameras and industrial software that limits video and processing functionalities dedicated to homeotherms beings, harming its application for diagnostic purposes.

Video thermometry together with a SaMD with mechanisms of artificial intelligence and machine learning, has the potential to emerge as a significant tool for cancer detection, even being used during surgical procedures to provide real-time visualization of tumor margins to the medical team. However, its utilization is still limited, due to emerging technology.

The dynamic images in this study were referred to as video thermometric or video thermometry images. Based on this, the objective of this study was to detect distant metastases in canine mammary neoplasms.

2. MATERIALS AND METHODS

2.1. Sampling method

Twenty-one female dogs with palpable mammary nodules underwent total unilateral mastectomy. This study was approved by the animal ethics committee ID 432171-CEUA/UENF. As the inclusion criteria, female dog in reproductive phase, without weight or age restrictions, with one or more evident masses of adenomas, carcinomas, or their mixed variants were included in this study. These surgeries were combined with real-time, non-contact video thermometry examination, and the image capture was performed in a temperature-controlled surgical center maintained at 22±2°C. All visible tumor masses were sent for histopathological diagnosis, and twenty-five presumptive samples, guided by VTM, were collected for histopathological study. In three surgeries, multiple presumptive samples were collected, as shown in Table 1.

2.2. Anesthetic Procedure

After trichotomy, the animal was taken to the operating room, where it was positioned, sedated, and anesthetized. Induction was performed by intravenous administration of propofol at a dose of 3 mg/kg^{-1}, and anesthesia maintenance was achieved with 100% oxygen and isoflurane via a semi-closed inhalation anesthesia circuit (Baraka system) for animals weighing up to 7 kg, and a semi-closed circuit for animals weighing over 7 kg. Intraoperative pain control was achieved through continuous infusion of morphine sulfate at a rate of 1.66 µg/kg-1/min, lidocaine hydrochloride at 30 $µg/kg^{-1}$/min, and ketamine hydrochloride at 15 $µg/kg^{-1}$/min, initially administered as bolus doses and subsequently maintained using an infusion pump at a dosage of 0.4 mg/kg of morphine, 1 mg/kg of lidocaine, and 1 mg/kg of ketamine. Heart rate (HR), respiratory rate (RR), peripheral oxygen hemoglobin saturation (SpO_2), electrocardiographic tracing, plethysmography, end-tidal carbon dioxide concentration ($EtCO_2$), and non-invasive blood pressure were monitored. The animals remained under spontaneous ventilation throughout the operation. Postoperative analgesia was achieved through a combination of oral tramadol hydrochloride at a dose of 4 mg/kg-1 every 12 hours, oral carprofen at a dose of 2.2 mg/kg^{-1} every 12 hours, and dipyrone at a dose of 25 mg/kg^{-1} every 12 hours, all administered for a duration of 5 days. Patient selection was based on clinical assessment and complementary exams (medical history, physical examination, laboratory tests, imaging exams, prescription of supportive care, and surgical referral), as well as postoperative care (hospitalization, monitoring, antibiotic therapy, and pain management).

2.3. Transoperative Video Thermometric Evaluation

The examination was performed using the MART (Metabolic Activity in Real-Time) station designed for surgical center and/or educational purposes, utilizing the Mart v2.0 software for video thermometric image processing and enhancement. The operator of the station was positioned outside the sterile environment, avoiding interference with the surgical routine, while the thermic sensor was positioned above the surgical field at a variable height ranging from 1 to 1.20 meters.

After sedation, a 15 minutes period was performed for the patient's thermal acclimatization with room temperature of 22±2°C before starting the inspection protocol. Subsequently, a provocative test was performed with 0.5% chlorhexidine alcoholic solution. This procedure helps to mark the main tumor

irrigation and the direction of blood flow in the mammary chains, axillary and inguinal lymph nodes to confirm, later, if images of similarity are found in the direction of the verified flow. As the skin generates heat, thermal discrepancies between nearby pixels call attention to dysfunction, perforating arteries, hot or cold regions for another reason and artifacts which must be differentiated during the exam.

2.4. Analysis of Video thermometric Images

In this experiment, in the pre-operative inspection, the “Merlin” tool, shows several small images with different color gradients, where the operator chooses the screen that shows the best image and transfer it to the processing area. In this sense, the operator processed the image following the MART protocol with the following routine: 1) assessment of symmetry; 2) vascular inspection; 3) analysis of thermal discrepancy in nearby pixels in areas suspected of abnormalities. 4) identification of textures and anatomical delimitation; 5) search for similarities of thermal patterns; when the operator marks a breast cancer known area and activate the “Similarity” tool, automatically identifies areas with the same thermal signature, thus enabling the identification of possible areas to be inspected by the surgeon during the surgical procedure. The operator suggest which presumptive samples should be collected in the preoperative. In this study, the images were recorded on video, in real time, from the acclimatization period until the beginning of the surgery[32,33].

3. RESULTS

In this study 21 unilateral total mastectomy surgeries were performed, and during these procedures, 23 presumptive samples of remote alterations were collected (Table 1).

Table 1. Identification of the number of surgeries and number of presumptive samples collected, histopathological diagnosis of the primary tumor, and remote presumptive samples in mammary tumors in female dogs.

PRIMARY TUMOR		PRESUMPTIVE RESULT
01	Carcinoma sólido	Breast Carcinoma Embolus and Vascular Hamartoma
02	Adenocarcinoma with Solid and Tubular Areas	Neoplastic Embolus in Vessel, Mammary Duct with Cellular Proliferation
03	Multicentric Tubular Carcinoma	Tubular Carcinoma
04	Solid Tubular Carcinoma	Tubular Carcinoma
05	Tubular Breast Adenocarcinoma	Tubular Breast Adenocarcinoma
06	Complex Adenomyoepithelioma	Malignant Grade II Adenomyoepithelioma
07	Complex Adenomyoepithelioma	Basal Cell Carcinoma, well-differentiated with clear surgical margins. Dermatitis.
08	Complex Adenocarcinoma with Differentiated Cystic and Papillary Areas	Mammary Cysts and Hyperplasia Mammary Hyperplasia
09	Tubular Carcinoma in Mixed Tumor	Lipoma Dermatitis
10	Solid Carcinoma	Dermatitis
11	Breast Adenoma	Breast Hyperplasia
12	Solid Carcinoma	No abnormalities detected
13	Suppurated Grade I Ductal Adenocarcinoma	No abnormalities detected
14	Complex Adenomyoepithelioma	No abnormalities detected
15	Cystadenocarcinoma in Mixed Tumor, Grade I and II	No abnormalities detected
16	Ulcerated Carcinosarcoma	No abnormalities detected
17	Papillary Adenocarcinoma	No abnormalities detected
18	Cystic and Papillary Adenocarcinoma with Abundant Squamous Differentiation	No abnormalities detected
19	Solid Adenocarcinoma	No abnormalities detected
20	Carcinoma in Mixed Tumor	No abnormalities detected
21	Tubular Carcinoma	No abnormalities detected

Of the collected samples, 07 neoplastic alterations and 06 non-neoplastic alterations were found. 10 samples had no alteration (Table 1). Among the altered samples, proven through histopathology, 44% were not detected by the conventional identification method, and 56% were not visible or palpable. All altered samples were found by video thermometry (Figure 3).

Of the total number of lesions identified, the evaluation performed using videotermometria was 62% more accurate than the conventional method (Figure 4).

In figure 5, it is possible to observe the demarcation of two known tumor masses, which are visible and palpable in the female dog abdominal and caudal breast. it is also possible to observe the thermal signature identification tool of the algorithm, which it was able to identify the two predominant temperatures, and similar ones, of the tumor masses already identified by the conventional method. However, the algorithm was also able to identify a cranial image with thermal impression similar to known masses, along the vascular pathways of the left mammary chain, with temperature discrepancy of the surrounding areas. This image, although very small, had the same thermal signature as the already known masses and, through histopathological examination, the presumed sample resulted in a neoplastic embolus.

In figure 6, it is possible to observe the visible tumor mass of the breast female dog, showing the previous left total mastectomy scar. In the video thermometry exam, it was possible to observe the textures of the tumor architecture, as well as the predominant vascular supply (black). Through the similarity analysis of the thermal signature, it was possible to identify an image in the right cranial abdominal mammary region, compatible with the vascular pathways and showing a thermal impression similar to the known mass, after the analysis and verification of the thermal discrepancies (red arrow). Through histopathological examination, the presumptive sample resulted in a neoplastic embolus compatible with carcinoma and vascular hamartoma.

In Figure 7A, it was possible to observe a visible solid tumor mass of adenocarcinoma in the right caudal abdominal breast. Next to it, the right inguinal mammary gland appears enlarged in relation to the contralateral gland, but on palpation, its elastic and deformable appearance suggests a lipoma. Figure 7B shows the intraoperative view of the right total mastectomy, where the tubular images become apparent.

Images 8C, 8D and 8E are from the intraoperative phase in which it is possible to observe the surgeon's hand over the tumor mass on the left. In the area marked with a red circle, three sequential moments were captured by VTM, revealing the ability of the technique, together with the algorithm, to highlight textures and tubular structures. Upon histopathological examination, the findings resulted in mammary hyperplasia and cysts.

4. DISCUSSION

Thermometry is an image generated by convert infrared radiation emitted from the body into electrical impulses (radiometric image) that are displayed on a monitor in various colors[34]. The spectrum of

colors based on a degrees scale indicates an increase or decrease in the infrared radiation or temperature being emitted from the body surface. An abnormality detected by thermal image indicates an area of temperature asymmetry in the body. Based on patterns of heat and blood flow on or near the surface of the body, thermometry has been utilized in an effort to detect, characterize, and monitor multiple diseases processes. Although thermography has already been demonstrated as a potential breast cancer detection mechanism[35,36,37], VTM can become an important tool during image processing, through an AI system capable of detecting benign alterations and distant metastases, tumor textures and delimitation, tumor vascular supply, as demonstrated by the data of this study.

Presumptive samples without abnormalities may be artifacts, vascular changes, or initial pathological changes not found on histopathological examination. This image reflects a different generation of heat from the surroundings, demonstrating that the composition of matter in this location generates a molecular movement that differs from the surrounding region.

According to Jiang et al., (2010), the dynamic state of the breast exhibits distinct patterns, which makes it difficult to identify thermal signatures to identify tumors and metastases in the tissue[38]. A study by Jawzal (2018) indicates that thermography reflects, mainly, a heat map under the skin, but does not exactly locate the tumor for surgical purposes, and may cause confusion during the procedure, when the metabolic intensity of some tumors decreases.

The results found in this study, with the advancement of technology, ~~are in~~ contrast to those found by Jiang et al., (2010) and Jawzal (2018), since, among all the samples with alteration that were verified in the study, 62% were alterations neoplastic lesions distant from the primary tumor (Figure 4). This result is promising, as benign and malignant lesions that would not be detected by the conventional method were identified by VTM.

It is noteworthy that the identification of distant metastases was made through the use of thermal signatures of the tumor tissue. This data shows the efficiency not only of the VTM, but also the algorithm, which was able to identify the thermal signatures of the lesion and detect the same signature, enabling the detection of distant metastases from the primary tumor, even at a very early stage.

Another factor that may explain the success rate of the technique in this study was reported by Vardasca et al., (2018), in which it was demonstrated that temperature differences between the areas of lesions and the surrounding tissue can be used to differentiate neoplasms. In the case of benign neoplasms of the skin, if dynamic thermal imaging (DTI) and application of cold stress are used, sensitivity and specificity values of 95% and 83%, respectively, were observed.[39]. According to Sadeghi et al., (2019), both stationary and dynamic infrared images can detect a superficial tumor, but in dynamic exams they can considerably increase efficiency, due to their increased contrast and thermal events, providing greater specificity and allowing analyze different tumor depths, after cold provocative tests[40]. These data corroborate those found in this study.

The potential of invisible thermal radiation is far from being fully exploited, as small variations in temperature distribution may go undetected and minimal discrepancies may be masked and remain undetected, due to two factors: low efficiency of thermal image capture sensors and thermal image treatment software[41]. It is known that computing is no longer a limitation in the processing of large volumes of data and algorithms for image segmentation have been the object of attention. The infrared systems developed in the 1970s and 80s are excellent for industrial or military purposes, but may not meet the needs of medical imaging applications, because for these high-precision images to reach their potential, minimum hardware requirements are required needed in the clinical environment[42]. James et al., (2014) demonstrated that the integration between hardware and software ends up being a limiting factor for the processing and storage of the infrared image in real-time [43], Singh et al., (2019), point out in their study that existing intelligent systems need to improve the commercially viable interface to serve users and validate the diagnosis.

In this sense, it can be noted that the results found in this study are based on the efficiency between the algorithm interaction with the operator experience (Figure 5 and 6). Therefore, despite being in constant evolution, the efficiency of the AI in detecting similar thermal signatures indicates a great step forward for the use of video thermometry in the detection of tumors and distant metastases, making possible the formation of a database (Machine Learning) for the identification of lesions and artifacts, possibly being this one of the main differentials of the results found in this study, in relation to the others.

According to Hodorowicz et al., (2020), the use of thermography for the purpose of early detection of breast cancer showed higher efficiency than those found in other commonly used techniques, even when combined[44]. These same researchers show that despite the encouraging results found, there is still a long way to go, especially in the use of intelligent software for detecting the thermal variations emitted by tumors. These data corroborate those found in this study (Figure 5, 6, 7 and 8).

It is known that VTM inspection looks for textures, vascular formations, known tumor thermal impression and similar areas in relation to the surroundings indicative of dysfunction. We also know that heat comes from molecular movement, respecting the degree of freedom of each molecule, tissue, organ, fluid and, since each compound has its own emissivity, then, the logic, applied to homeotherms, should be better understood. Different metabolic intensities in nearby pixels, or thermal impressions similar to tumors at a distance, in a thermally controlled environment, are not a natural condition and, as homeotherms do not tend towards thermal equilibrium as materials do, both heat production and heat loss have the purpose of keeping the temperature stable, since most of the enzymes responsible for metabolic functioning act effectively at this temperature[45].

Most natural surfaces form repetitive patterns of texture that can be recognized and differentiated by the human eye through characteristics such as smoothness, roughness and regularity[46]. Furthermore, a universal algorithm for image segmentation certainly does not exist[47], but texture and shape can show organs, tissues and anomalies, which in most cases have specific textures and shapes[48], therefore, software and algorithms can guide us in the range of the invisible and, if we consider that the

occurrences are happening, we can say that the information is available and it is up to us to find ways to access it. Based on this, it is important to emphasize that this study was able to detect textures and thermal signatures (Figure 7 and 8). Despite an initial study, the data demonstrate an evolution between the thermometric data and the generated image, reducing the dependence on exclusive thermal analysis, since the image starts to bring more visual information and a big step towards understanding heat signatures for medical use.

5. CONCLUSION

In this study, it was possible to observe the VTM assertive capacity in identifying distant metastases and breast tumors in female dogs, in relation to conventionally used techniques. It was also possible to identify textures with anatomical limits, emboli to early formations of carcinomas, adenocarcinomas and adenomyoepithelioma. It was also possible to find non-neoplastic changes such as dermatitis, lipoma, hyperplasia and breast cysts. It can be seen that these lesions would not be identified in conventional surgical planning, as the presumptive samples were not visible or palpable, being video guided exclusively by VTM. This result is promising, as benign and malignant lesions that would not be detected by the conventional method were identified by VTM, initiating the identification of lesions and artifacts for the formation of a database (Machine Learning) in order to increase accuracy. It can be concluded that the videothermometry exam is a promising technology in the preoperative evaluation of breast cancer and surgical planning, having the potential to be a routine exam and increase its applicability.

Declarations

ACKNOWLEDGEMENTS

Ao Department of Clinical Surgery Veterinary Hospital of Universidade Estadual do Norte Fluminense Darcy Ribeiro (UENF) and to all professionals involved in this department.

To Galzu Institute, Rio de Janeiro, Brazil, for the assignment of the MART station.

CONFLICT OF INTEREST

All of the authors claim that no conflict of interest exists.

References

1. Kristiansen, V. M., Nødtvedt, A., Breen, A. M., Langeland, M., Teige, J., Goldschmidt, M., & Sørenmo, K. (2014). Effect of ovariohysterectomy at the time of tumour removal in dogs with benign mammary tumours and hyperplastic lesions: a randomised controlled clinical trial. European Journal of Companion Animal Practice, 24(1), 56-66.
2. Ward, L. S. (2002). Entendendo o processo molecular da tumorigênese. Arquivos Brasileiros de Endocrinologia & Metabologia, 46(4), 351-360.

3. Gamagami P: Indirect signs of breast cancer: Angiogreneis study. In: Atlas of Mammography, Cambridge, MA: Blackwell Science, pp, 231- 258, 1996.
4. Maji, S., Chaudhary, P., Akopova, I., Nguyen, P. M., Hare, R. J., Gryczynski, I., & Vishwanatha, J. K. (2017). Exosomal annexin II promotes angiogenesis and breast cancer metastasis. Molecular Cancer Research, 15(1), 93-105.
5. Guidi AJ and Schnitt SJ: Angiogenesis in preinvasive lesions of the breast. The Breast J2: 364-369, 1996.
6. Li, C. Y., Shan, S., Huang, Q., Braun, R. D., Lanzen, J., Hu, K., ... & Dewhirst, M. W. (2000). Initial stages of tumor cell-induced angiogenesis: evaluation via skin window chambers in rodent models. Journal of the National Cancer Institute, 92(2), 143-147.
7. Mccarty, Mark F.; WHITAKER, Julian. Manipulating tumor acidification as a cancer treatment strategy. Altern Med Rev, v. 15, n. 3, p. 264-72, 2010.
8. Sun-wada, Ge-Hong; Wada, Yoh. Role of vacuolar-type proton ATPase in signal transduction. Biochimica et Biophysica Acta (BBA)-Bioenergetics, v. 1847, n. 10, p. 1166-1172, 2015.
9. Hinton, A., Sennoune, S. R., Bond, S., Fang, M., Reuveni, M., Sahagian, G. G., ... & Forgac, M. (2009). Function of a subunit isoforms of the V-ATPase in pH homeostasis and in vitro invasion of MDA-MB231 human breast cancer cells. Journal of Biological Chemistry, 284(24), 16400-16408.
10. Yahara, T., Koga, T., Yoshida, S., Nakagawa, S., Deguchi, H.: Relationship between microvessel density and thermographic hot areas in breast cancer Surg Today (2003) 33, 243-248
11. Çengel, Yunus A.; Ghajar, Afshin J. Tranferência de calor e massa. AMGH Editora, 2009. P42
12. Bagavathiappan, S. et al. Infrared thermography for condition monitoring–A review. Infrared Physics & Technology, v. 60, p. 35-55, 2013.
13. Houdas, Y.; Ring, R. F. J. Human Body Temperature - Its Measurements And Regulation. New York, Plenum, 1982.
14. B. W. C. Amalu, “A review of breast thermography,” Int. Acad. Clin. Thermol., p. 112, 2003.
15. J. Steketee, Spectral emissivity of the skin and pericardium, Physics in Medicine & Biology 18 (1973) 686–694.
16. Peeters, J., Louarroudi, E., Bogaerts, B., Sels, S., Dirckx, J. J. J., & Steenackers, G. (2018). Active thermography setup updating for NDE: a comparative study of regression techniques and optimisation routines with high contrast parameter influences for thermal problems. Optimization and Engineering, 19(1), 163-185.
17. Jawzal; H.; & Ekici; S. Trends in Breast Cancer Screening Using Thermography: A Review (2018). International Journal of Latest Technology in Engineering; Management & Applied Science (IJLTEMAS) Vol. VII; Issue V.
18. Mendelsohn, R., Flach, C. R., & Moore, D. J. (2006). Determination of molecular conformation and permeation in skin via IR spectroscopy, microscopy, and imaging. Biochimica et Biophysica Acta (BBA)-Biomembranes, 1758(7), 923-933.

19. Sanches, I. J., Gamba, H. R., Souza, M. A. D., Neves, E. B., & Nohama, P. (2013). Fusão 3D de imagens de MRI/CT e termografia. Revista Brasileira de Engenharia Biomédica, 29(3), 298-308.
20. Usamentiaga; R.; Venegas; P.; Gueredíaga; J.; Vega; L.; Molleda; & Bulnes; F. G. (2014). Infrared thermography for temperatur; 14(7); 12305-12348.
21. Bianco, A. C. (2000). Hormônios tireóideos, UCPs e termogênese. Arquivos Brasileiros de Endocrinologia & Metabologia, 44(4), 281-289.
22. Niaz, M. (2006). Can the study of thermochemistry facilitate students' differentiation between heat energy and temperature?. Journal of Science Education and Technology, 15(3-4), 269.
23. Laburú, C. E., & Niaz, M. (2002). A Lakatosian framework to analyze situations of cognitive conflict and controversy in students' understanding of heat energy and temperature. Journal of Science Education and Technology, 11(3), 211-219.
24. Etehadtavakol, M., & Ng, E. Y. (2017). An overview of medical infrared imaging in breast abnormalities detection. In Application of infrared to biomedical sciences (pp. 45-57). Springer, Singapore.
25. Singh, D., & Singh, A. K. (2019). Role of image thermography in early breast cancer detection: Past, present and future. Computer methods and programs in biomedicine, 105074.
26. Pérez, M. G., Conci, A., Aguilar, A., Sánchez, Á., & Andaluz, V. H. (2014). Detección temprana del cáncer de mama mediante la termografía en Ecuador. Maskana, 5, 111-123.
27. S. Uematsu, Symmetry of skin temperature comparing one side of the body to other, Thermology 1 (1986) 4–7.
28. Hill, Derek Lg Et Al. Medical Image Registration. Physics In Medicine And Biology, V. 46, N. 3, P. R1, 2001.
29. Kandlikar, S. G., Perez-Raya, I., Raghupathi, P. A., Gonzalez-Hernandez, J. L., Dabydeen, D., Medeiros, L., & Phatak, P. (2017). Infrared imaging technology for breast cancer detection–Current status, protocols and new directions. International Journal of Heat and Mass Transfer, 108, 2303-2320.
30. Sadeghi, M., Boese, A., Maldonado, I., Friebe, M., Sauerhering, J., Schlosser, S., ... & Wehberg, K. (2019). Feasibility test of Dynamic Cooling for detection of small tumors in IR thermographic breast imaging. Current Directions in Biomedical Engineering, 5(1), 397-399.
31. Chebbah, N. K., Ouslim, M., & Benabid, S. (2023). New computer aided diagnostic system using deep neural network and SVM to detect breast cancer in thermography. *Quantitative InfraRed Thermography Journal*, *20*(2), 62-77.
32. Collins, A. J., & Ring, E. F. J. (1972). Measurement of inflammation in man and animals by radiometry. British journal of pharmacology, 44(1), 145.
33. Zhang, Z. M., Tsai, B. K., & Machin, G. (2009). Radiometric temperature measurements: I. Fundamentals. Academic press.
34. American College of Clinical Thermology. Overview of Digital Infrared Thermal Imaging. Available at: http://www.thermologyonline.org/ Patients/patients_overview.htm. Date posted: Not available.

Accessed March 3, 2017.

35. Arora, N., Martins, D., Ruggerio, D., Tousimis, E., Swistel, A. J., Osborne, M. P., & Simmons, R. M. (2008). Effectiveness of a noninvasive digital infrared thermal imaging system in the detection of breast cancer. *The American Journal of Surgery*, *196*(4), 523-526.
36. Wishart, G. C., Campisi, M., Boswell, M., Chapman, D., Shackleton, V., Iddles, S., ... & Britton, P. D. (2010). The accuracy of digital infrared imaging for breast cancer detection in women undergoing breast biopsy. *European Journal of Surgical Oncology (EJSO)*, *36*(6), 535-540.
37. Kennedy, D. A., Lee, T., & Seely, D. (2009). A comparative review of thermography as a breast cancer screening technique. *Integrative cancer therapies*, *8*(1), 9-16.
38. Jiang; L.; Zhan; W.; & Loew; M. H. (2010). Modeling static and dynamic thermography of the human breast under elastic deformation. Physics in Medicine & Biology; 56(1); 187.
39. Magalhaes, C., Vardasca, R., & Mendes, J. (2018). Recent use of medical infrared thermography in skin neoplasms. Skin Research and Technology, 24(4), 587-591.
40. González, F. J., González, R., & López, J. C. (2019). Thermal contrast of active dynamic thermography versus static thermography. Biomedical Spectroscopy and Imaging, 8(1-2), 41-45.
41. Neal, C. H., Flynt, K. A., Jeffries, D. O., & Helvie, M. A. (2018). Breast imaging outcomes following abnormal thermography. *Academic radiology*, *25*(3), 273-278.
42. Fauci, M. A., Breiter, R., Cabanski, W., Fick, W., Koch, R., Ziegler, J., & Gunapala, S. D. (2001). Medical infrared imaging–differentiating facts from fiction, and the impact of high precision quantum well infrared photodetector camera systems, and other factors, in its reemergence. Infrared physics & technology, 42(3-5), 337-344.
43. James, Alex Pappachen; Dasarathy, Belur V. Medical Image Fusion: A Survey Of The State Of The Art. Information Fusion, V. 19, P. 4-19, 2014.
44. Hodorowicz-Zaniewska, D., Zurrida, S., Kotlarz, A., Kasprzak, P., Skupień, J., Ćwierz, A., ... & Basta, P. (2020). A prospective pilot study on use of liquid crystal thermography to detect early breast cancer. *Integrative Cancer Therapies*, *19*, 1534735420915778.
45. Braz, José Reinaldo Cequeira. Fisiologia da termorregulação normal. Revista Neurociências, v. 13, n. 3, p. 12-7, 2005.
46. Tuceryan, Mihran et Al. Texture Analysis. Handbook Of Pattern Recognition And Computer Vision, V. 2, P. 235-276, 1993.
47. Pham, Dzung L.; Xu, Chenyang; Prince, Jerry L. Current Methods In Medical Image Segmentation. Annual Review Of Biomedical Engineering, V. 2, N. 1, P. 315-337, 2000.
48. Balan, Agr Et Al. Fractal Analysis Of Image Textures For Indexing And Retrieval By Content. In: Computer-Based Medical Systems, 2005. Proceedings. 18th IEEE Symposium On. IEEE, 2005. P. 581-586.

Figures

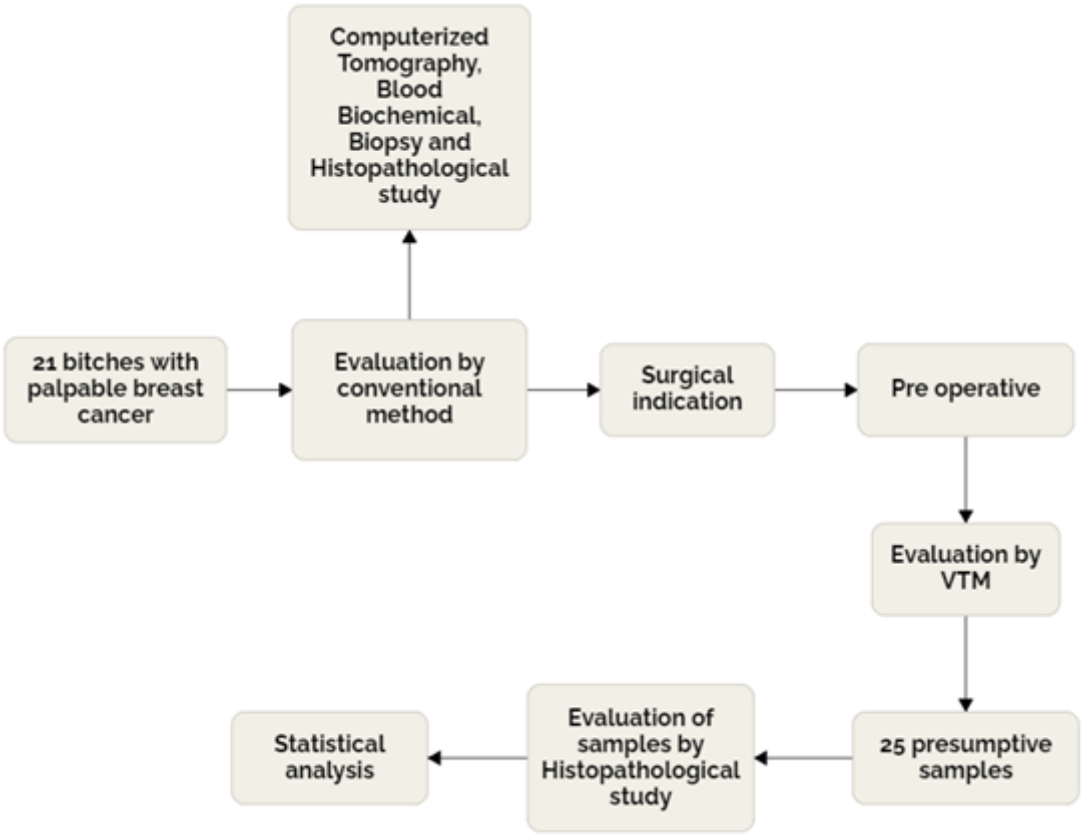

Figure 1

Participation flowchart.

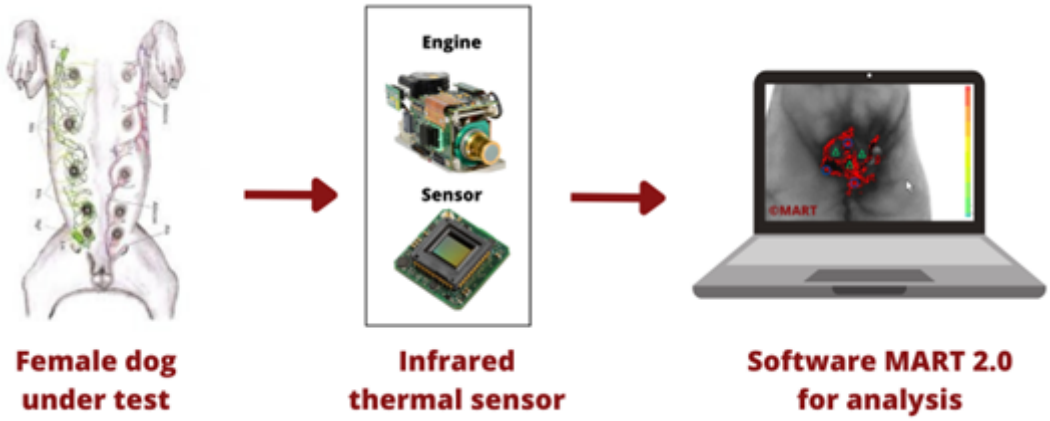

Figure 2

Female dog breast thermometry procedure.

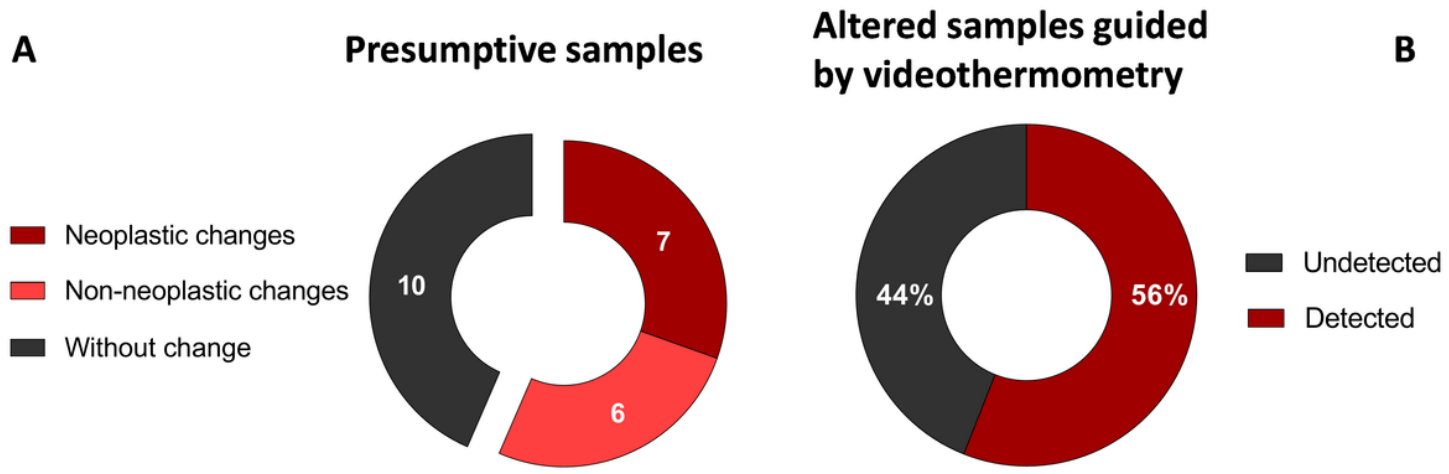

Figure 3

A) Total number of presumptive samples collected and analyzed. B) Percentage of samples detected by the VTM technique in relation to the traditional method.

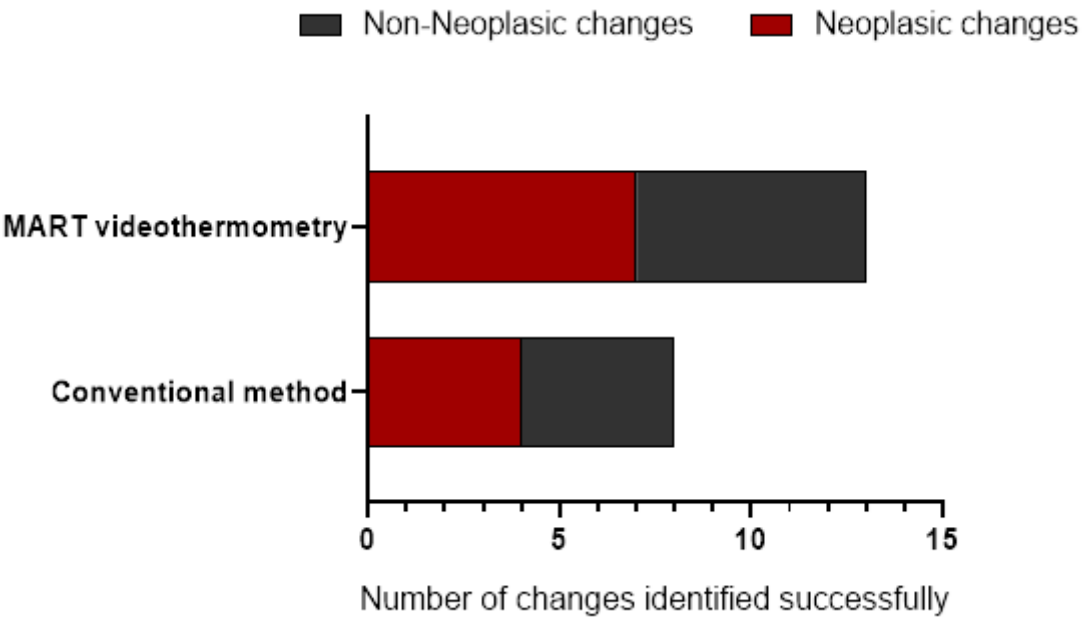

Figure 4

Total number of tumor samples successfully identified by the techniques used.

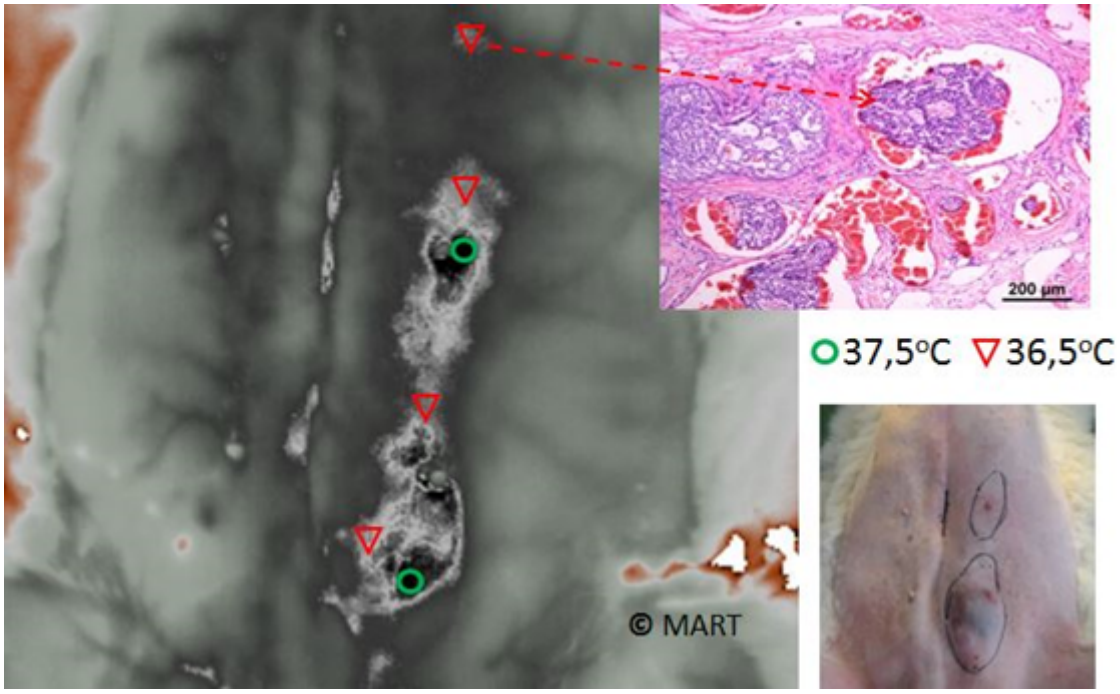

Figure 5

Demarcation of tumor mass and identification of non-visible or palpable distant metastasis, identified by VTM (red and green markings).

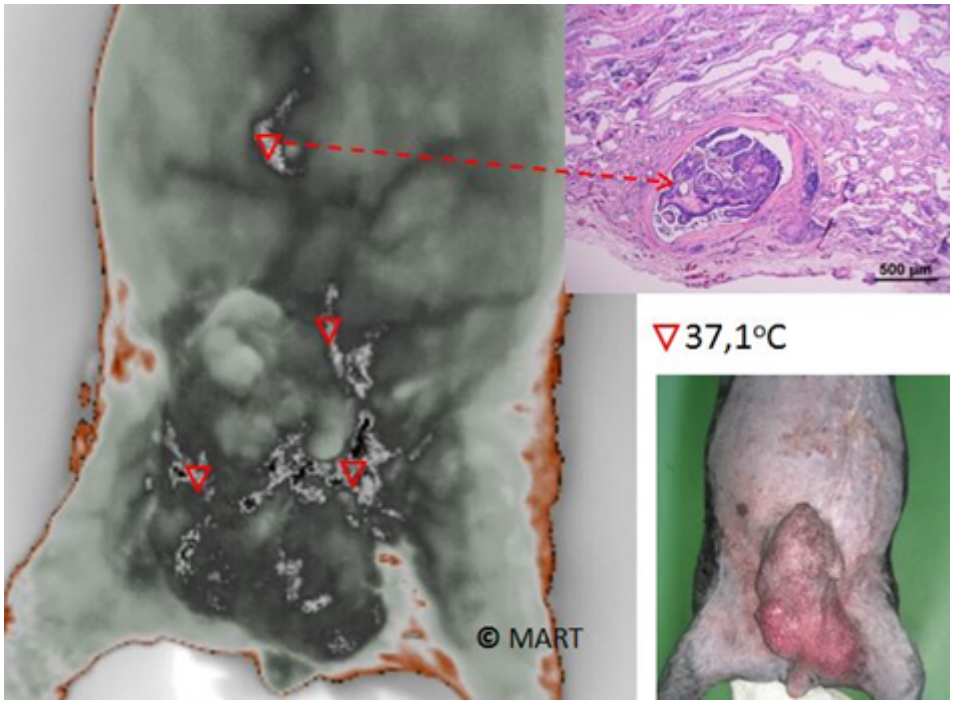

Figure 6

Demarcation of tumor mass and identification of non-visible or palpable distant metastasis, identified by VTM (red markings).

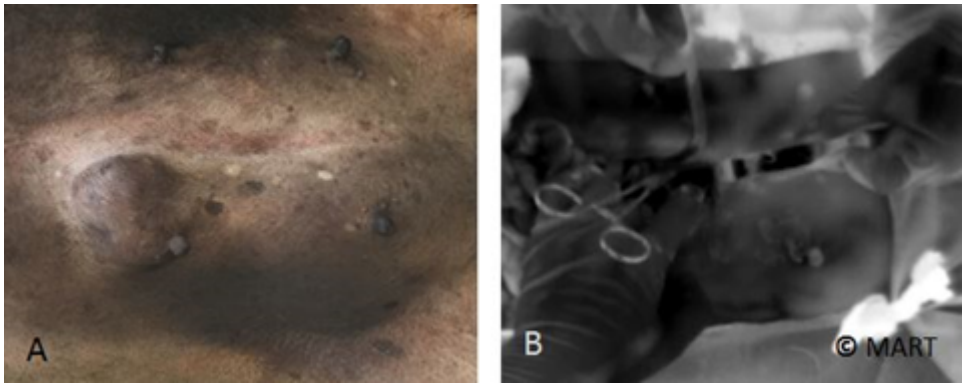

Figure 7

Mammary tumor in a female dog. In image A, we observe the real image of a visible solid tumor mass of adenocarcinoma in the right caudal abdominal mammary gland.

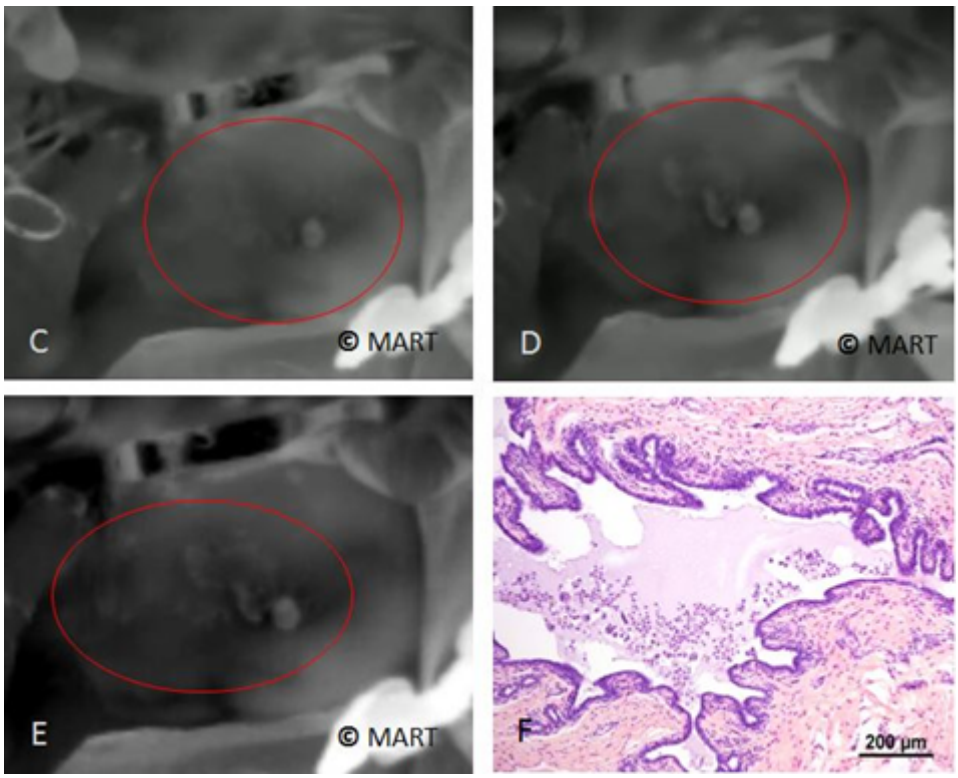

Figure 8

Images C, D, and E demonstrate sequential moments were captured by VTM, revealing textures that highlight tubular structures.